

Volumetric Properties, Viscosities, and Isobaric Heat Capacities of Imidazolium Octanoate Protic Ionic Liquid in Molecular Solvents

Mérièm Anouti,* Johan Jacquemin, and Daniel Lemordant

Université François Rabelais de Tours, Laboratoire PCMB (EA 4244), Équipe Chimie de Physique des Interfaces et des Milieux Electrolytiques (CIME), Parc de Grandmont, 37200 Tours, France

Densities (ρ), viscosities (η), and isobaric heat molar capacities (C_p) of binary mixtures containing imidazolium octanoate, [Im][C₇CO₂], a protic ionic liquid (PIL), with four molecular solvents, water, acetonitrile, ethanol, and 1-octanol, are determined as a function of temperature from (298.15 to 323.15) K and within the whole composition range at atmospheric pressure. Excess molar volumes, V^E , excess molar heat capacities, C_p^E , and the deviation from additivity rules of viscosities, $\Delta\eta$, of imidazolium octanoate solutions were then deduced from the experimental results, as well as apparent molar volumes, $V_{\phi i}$, and partial molar volumes, $\bar{V}_{m,i}$. Results are discussed according to the nature of the interaction between the PIL and the molecules and the effect of temperature. The excess Gibbs energies of activation of viscous flow (ΔG^{*E}) for these systems were then calculated at 298.15 K. The excess isobaric heat capacities, C_p^E , of binary ([Im][C₇CO₂] + solvent) systems, depend also of the nature of the molecular solvent in mixture. The excess properties were then correlated, at each temperature, as a function of composition by a Redlich–Kister-type equation. Finally results have been discussed in terms of molecular interactions and molecular structures in these binary mixtures, and thermodynamic properties of investigated binary mixtures were then compared to literature values together to investigate the impact of the nature of the solvent on these reported properties.

Introduction

Ionic liquids (ILs) are organic salts, liquids at temperatures below 100 °C. Because of their unique chemical and physical properties—including stability on exposure to air and moisture, a high solubility power, and extremely low vapor pressure—ILs can serve as new solvents for catalysis, synthesis, and extraction as an alternative to volatile organic compounds, which are traditionally used in industrial processes.^{1–6} For this reason, they rapidly gained interest as greener replacements for traditional volatile organic solvents (VOCs). ILs are generally constituted by an organic cation and organic or inorganic anion; those formed by the transfer of a proton between a Brønsted acid and a Brønsted base form a protic subgroup in the class of ambient temperature fluid systems, now referred as “protic ionic liquids” (PILs). To date, PILs have not received a particularly large share of the literature based on IL studies.⁷ Nevertheless, this IL family has many useful properties and potential applications, often arising from their protic nature, including as self-assembly media,^{8–12} reaction media and catalysts for organic reactions,^{13–15} biological applications,^{16–18} proton conducting electrolytes for polymer membrane fuel cells,^{19–21} and explosives.^{22,23}

In spite of the importance of IL properties in aqueous or nonaqueous solutions, there is limited information available on the thermodynamic properties of IL mixtures with other fluids and these properties still lacking.^{24–26} There are many experimental and theoretical studies, which deal on the behavior of thermodynamic properties of mixtures containing IL with common organic solvents.^{27–31} However, because of the enormous number of possible binary systems, a lot of work

remains to be done. Many efforts in this field have been devoted to the study of (room-temperature ionic liquid (RTIL) + water) and (RTIL + alcohol) binary systems, mainly motivated by solubility of ILs in these molecular solvents as well as the low environmental impact of these mixtures.^{30,32}

In recent years, ILs based on the 1-alkyl-3-methylimidazolium cation ([C_nmim]⁺) have received much attention.³³ An interesting aspect of these types of ILs is that the [C_nmim]⁺ cations possesses inherent amphiphilic character when the alkyl group is a long hydrocarbon chain.²⁶ In solution, the solvation and the interactions of the ions or ion pairs with the solvent determine the unique properties of these systems.³⁴ The volumetric properties of electrolyte and nonelectrolyte solutions have been particularly informative in elucidating the solute–solvent and solute–solvent interactions that exist in these solutions.

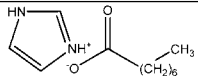
We have studied in previous work the good micellar properties of new class of PILs based on the imidazolium cation with carboxylates as a counteranion.³⁵ To continue this work, we present herein thermodynamic and transport properties of imidazolium octanoate in molecular solvents.

The aim of this work is to study density (ρ), viscosity (η), and isobaric heat capacity (C_p) of imidazolium octanoate PIL in a mixture with molecular solvents as water, alcohols (ethanol and 1-octanol), and acetonitrile. η and C_p have been measured at several temperatures from (298.15 to 323.15) K, and ρ was measured at 298.15 K.

The excess properties were calculated and then correlated, at each temperature, as a function of composition by a Redlich–Kister-type equation. The apparent and partial molar volumes of the investigated PIL solutions have been evaluated as a function of concentration. Limiting partial molar volumes at infinite dilution have been then determined. Finally, the thermodynamic properties of investigated binary mixtures

* Corresponding author. E-mail: meriem.anouti@univ-tours.fr. Fax: (33)247367360. Tel.: (33)247366951.

Table 1. Characteristics of Imidazolium Octanoate PIL at 298.15 K: Molar Mass (M), Density (ρ), Molar Volume (V_m), Viscosity (η), Ionic Conductivity (σ), Molar Conductivity (Λ), and Surface Tension (γ)³⁵

Imidazolium octanoate [Im][C ₇ CO ₂]	M g·mol ⁻¹	ρ g·cm ⁻³	V_m cm ³ ·mol ⁻¹	η mPa·s	σ mS·cm ⁻¹	Λ S·cm ² ·mol ⁻¹	γ mN·m ⁻¹
		± 0.2 %	± 0.1 %	± 2 %	± 2 %	± 2 %	± 4 %
	212.15	0.9870	214.94	76.5	0.621	0.1335	32.8

containing the selected PIL were then compared together to investigate the impact of the nature of the solute on these reported properties.

Experimental Section

Materials and Methods. Octanoic acid ($\geq 99\%$) and imidazole ($\geq 99.5\%$) used into this study are commercially available (Sigma-Aldrich) and were used without further purification. The ¹H NMR spectrum of the PIL is obtained using a Bruker 200 MHz spectrometer, with CDCl₃ as solvent and tetramethylsilane (TMS) as an internal standard.

Double-distilled deionized water was used for the preparation of aqueous solutions. Ethanol ($\geq 99\%$), 1-octanol ($\geq 99\%$), and acetonitrile are commercially available (Sigma-Aldrich). Binary mixtures containing the PIL and molecular solvent were prepared by mass with an accuracy of $\pm 1 \cdot 10^{-4}$ g using a Sartorius 1602 MP balance. The densities of pure components and their mixtures were measured using a pycnometer immersed in a thermostatted bath. The uncertainty for densities did not exceed $\pm 0.02\%$. The temperature was measured by using a 100 Ω platinum resistance thermometer within an accuracy of ± 0.1 K. A differential scanning calorimeter (Perkin-Elmer DSC6) was used to obtain the isobaric heat capacities of the pure components and investigated mixtures. The measuring and the reference cells were filled with inert aluminum pans. All differential scanning calorimetry (DSC) measurements were performed under a N₂ atmosphere with the heating rate of 5 K·min⁻¹. The isobaric heat capacities were calculated from heat flow (mW) and the scan rate (K·mn⁻¹) for each sample (mg). The uncertainty of each calculated isobaric heat capacities did not exceed $\pm 1.5\%$. Viscosities were measured using a TA Instrument rheometer (AR 1000) with a conical geometry at various temperatures (from (293.15 to 323.15) K) at shear rate $\omega = 20$ s⁻¹ during heating and cooling runs. The uncertainty of each measured did not exceed $\pm 0.1\%$.

Preparation of Imidazolium Octanoate PIL. The synthesis and physicochemical properties of imidazolium octanoate are reported by our group in a previous paper.³⁵ Its synthesis has been resumed as following:

Imidazole (95.49 g; 1.40 mol) is placed in a three-neck round-bottomed flask immersed in an ice bath and equipped with a reflux condenser, a dropping funnel to add the acid, and a thermometer to monitor the temperature. Under vigorous stirring, octanoic acid (205.41 g; 1.42 mol) is added dropwise to the imidazole (during 1 h). The mixture temperature is maintained at less than 298.15 K during the addition of the acid by using an ice bath. Stirring is maintained for 4 h at ambient temperature, and a noncolored and low-viscous liquid is obtained. The residual octanoic acid is evaporated under reduced pressure, and the remaining liquid is further dried at 386 K under reduced pressure (0.1 Pa) to obtain the PIL (78.59 g; 98.7%). Since PILs are very hygroscopic compounds, imidazolium octanoate

was dried overnight at 353 K under high vacuum (0.1 Pa) prior to use. The PIL is analyzed for water content using coulometric Karl Fischer titration prior to all measurements. The water content in the PIL, measured after treatment, is close to 60 ppm (0.006 % w_w). To preserve this moisture-sensitive compound, the imidazolium octanoate is then placed into a desiccator containing desiccants like P₂O₅. After a few weeks, the water content in this PIL was then remeasured, and water content in this PIL was close to 800 ppm (0.08 % w_w). The PIL is characterized by linear voltammetry, DSC, and ¹H NMR spectrometry. These characterizations are presented in the Supporting Information.

Physicochemical properties at 298.15 K of imidazolium octanoate, denoted [Im][C₇CO₂], are listed in Table 1.

Results and Discussion

The volumetric properties of ([Im][C₇CO₂] + solvent) mixtures are described in this section.

Densities and Excess Molar Volumes. The density values, ρ , for ([Im][C₇CO₂] ($i = 1$) + solvent ($i = 2$)) mixtures, where the solvent is water, acetonitrile, ethanol, or 1-octanol, are measured at 298.15 K with an accuracy of (± 0.0002) g·cm⁻³. Results are listed in Tables S1 to S4 and presented in Figure S1 in the Supporting Information. Excess molar volumes, V^E , are then calculated according to the following equation:

$$V^E = \left[\frac{(x_1 M_1 + x_2 M_2)}{\rho} \right] - \left[\frac{x_1 M_1}{\rho_1} + \frac{x_2 M_2}{\rho_2} \right] \quad (1)$$

where x_i , M_i , and ρ_i are the mole fraction, the molar mass, and the density of component i , respectively.

Experimental V^E data of studied mixtures are listed in Tables S1 to S4 in the Supporting Information with an accuracy greater than 0.0005 cm³·mol⁻¹. Figure 1 shows negative excess molar volumes over the entire mole fraction range for PIL mixtures with water, ethanol, and acetonitrile. In the case of longest carbon chain alcohols such as 1-octanol, the V^E variations as a function of the composition describe positive deviations. Moreover, irrespective of the nature of the solvent in studied mixtures or of the sizes of the alkyl chain length in the case of alcohols, all excess molar volumes are limited (down to (0.5 to 2.0) cm³·mol⁻¹; corresponding to (0.2 to 1.3) % of the mixture's molar volume).

A more peculiar feature of these curves is their asymmetry, in other words, their V^E maximum localization in mole fraction of PIL composition. In the case of acetonitrile PIL solutions, V^E show a higher maxima at $x_1 = 0.7$, whereas for aqueous solution, the maxima is observed at $x_1 = 0.25$. In fact, asymmetrical curves of V^E are more likely to occur when the two components of the mixture have a large molar volume difference, as is indeed the case for water or acetonitrile. For

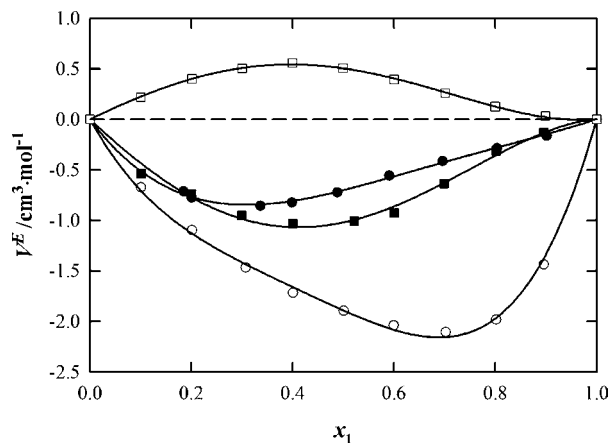


Figure 1. Comparison of excess molar volumes of binary mixtures of ([Im][C₇CO₂] + molecular solvent) at 298.15 K as a function of [Im][C₇CO₂] mole fraction composition, x_1 : ●, water; ○, acetonitrile; ■, ethanol; □, 1-octanol. The lines represent the Redlich–Kister-type fittings with the parameters indicated in the Table 1.

alcohols, the V^E curve is less symmetric with a maximum around $x_1 = 0.4$. It is known that in several binary mixtures containing ILs the locus of maxima or minima in V^E against composition is also away from the equimolar composition.^{36,37} Furthermore, several authors^{27,38,39} have measured the excess molar volumes of binary mixtures containing (IL + alcohol) for alkylsulfate-based, tetrafluoroborate-based, and bis(trifluoromethylsulfonyl)imide-based ILs, respectively, and their results exhibit asymmetric curves with negative-to-positive trends as the alcohol alkyl-chain length increases.

The excess molar volume, V^E , depends mainly on two factors: (i) variation in intermolecular forces between two components into contact and (ii) variation in molecular packing as a consequence of differences in size and shape of molecules. If interactions between unlike molecules are weaker than those between like molecules, excess molar volumes will be positive. This is the case of 1-octanol, which is responsible for specific interactions with the alkyl chain of the carboxylate anion, when the excess volume is positive. For the three other solvents, the interactions between unlike molecules are higher than those between like molecules that as a consequence negative V^E are observed by following this order: water < ethanol < acetonitrile. The effect of acetonitrile being most marked is due to electrostatic repulsion with the imidazolium ring of the cation in solution.

Apparent and Partial Molar Volumes. The apparent molar volumes of a component in the ([Im][C₇CO₂] ($i = 1$) + solvent ($i = 2$)) mixture $V_{\phi i}$ of PIL are defined as:

$$V_{\phi i} = \frac{V_m - x_j V_{m,j}}{x_i} \quad (2)$$

where V_m is the molar volume of mixture, x_i is the mole fraction of component i in the mixture, $V_{m,i}$ is the molar volume of the pure component i , and j is the second component. A combination of eqs 1 and 2 gives the following set of equations:

$$V_{\phi 1} = \left(V_{m,1} + \frac{V^E}{x_1} \right) \quad (3)$$

$$V_{\phi 2} = \left(V_{m,2} + \frac{V^E}{x_2} \right) \quad (4)$$

$V_{\phi 1}$ and $V_{\phi 2}$ values are reported in Tables S1 to S4 of the Supporting Information.

The partial and excess partial molar volumes have frequently been used to give insight on solute–solvent interactions. Therefore, the partial molar volume of the PIL in the mixture has been calculated using the following relation:

$$\bar{V}_{m,1} = V_{m,1} + \left(\frac{V^E}{x_1} \right) + x_1(1 - x_1) \left[\frac{\partial(V^E/x_1)}{\partial x_1} \right]_{P,T} \quad (5)$$

where $\bar{V}_{m,1}$ and $V_{m,1}$ are the partial molar volume of the PIL in solution and molar volume of the pure IL. The variations of the partial molar volume of the components $\bar{V}_{m,i}$ of the ([Im][C₇CO₂] + solvent) system at 298.15 K are reported in Tables S1 to S4. $\bar{V}_{m,1}$ and $V_{\phi 1}$ are plotted in Figure S2a–d. Figure S3 shows the evolution of the partial molar volumes $\bar{V}_{m,2}$ and $V_{\phi 2}$, against the PIL mole fraction, x_1 , for ([Im][C₇CO₂] + solvent) binary systems at 298.15 K for water (a), acetonitrile (b), ethanol (c), and 1-octanol (d) as solvents. In Figure 2, the partial molar volume $\bar{V}_{m,1}$ of the PIL in solution with all molecular solvents studied is reported for comparison. We note that, as expected, higher deviations from molar volumes of pure PIL are observed with acetonitrile mixtures.

Infinite dilution values ($\bar{V}_{m,1}^\infty$), reported in Table 2, were determined by graphical extrapolation of the variations of $V_{\phi i}$

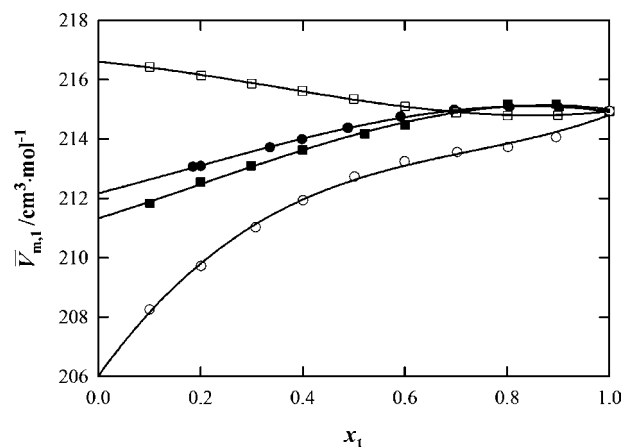


Figure 2. Partial molar volumes of [Im][C₇CO₂], $\bar{V}_{m,1}$, against the mole fraction of [Im][C₇CO₂], x_1 , for ([Im][C₇CO₂] + molecular solvent) at 298.15 K: ●, water; ○, acetonitrile; ■, ethanol; □, 1-octanol. The lines are just a guide to the eye.

Table 2. Partial Molar Volumes at Infinite Dilution, for [Im][C₇CO₂], $\bar{V}_{m,1}^\infty$, and Molecular Solvent, $\bar{V}_{m,2}^\infty$, and Molar Volumes $V_{m,i}$ of the Pure Liquids at 298.15 K

$\bar{V}_{m,1}^\infty$ cm ³ ·mol ⁻¹	$\bar{V}_{m,2}^\infty$ cm ³ ·mol ⁻¹	$V_{m,1}$ cm ³ ·mol ⁻¹	$V_{m,2}$ cm ³ ·mol ⁻¹
212.16	14.62	214.94	18.06
206.03	45.37	214.94	53.21
211.32	54.25	214.94	58.32
216.59	160.04	214.94	157.95

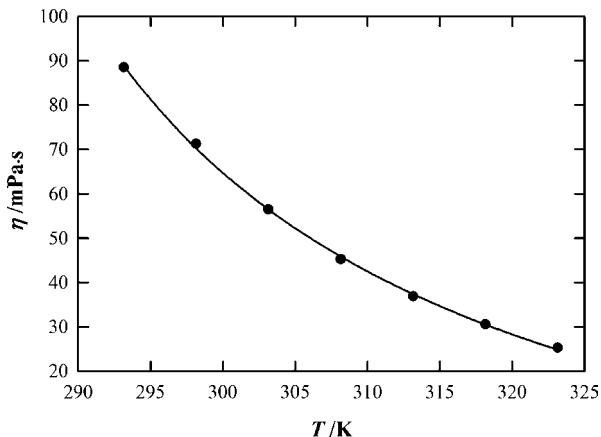


Figure 3. Viscosity, η , of $[\text{Im}][\text{C}_7\text{CO}_2]$, as a function of the temperature T from (293.15 to 323.15) K. The line represents the VTF-type fitting. The parameters are indicated into the text of the manuscript after eq 6.

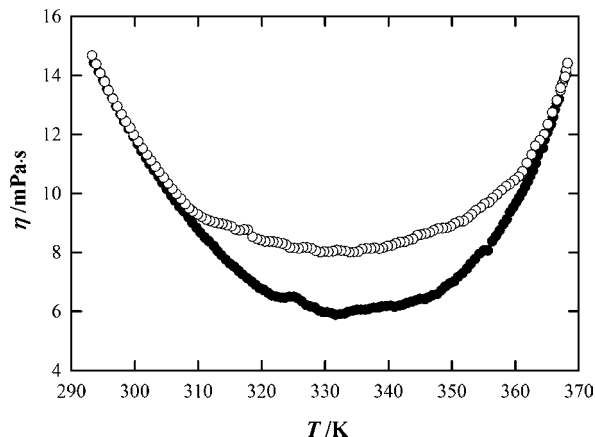


Figure 4. Temperature effect on the viscosity, η , of the ($[\text{Im}][\text{C}_7\text{CO}_2]$ + 1-octanol) mixture for a mole fraction of $[\text{Im}][\text{C}_7\text{CO}_2]$, $x_1 = 0.2$, as a function of the temperature T from (293.15 to 363.15) K. Viscosity data obtained by increasing, ●; and decreasing, ○; the temperature.

Table 3. Viscosities, η , and Viscosity Deviations from Ideality, $\Delta\eta$, for ($[\text{Im}][\text{C}_7\text{CO}_2]$ + Molecular Solvent) as a Function of $[\text{Im}][\text{C}_7\text{CO}_2]$ Mole Fraction Composition, x_1 , and Temperature up to 323.15 K

T/K	293.15		298.15		303.15		308.15		313.15		318.15		323.15	
	η	$\Delta\eta$	η	$\Delta\eta$	η	$\Delta\eta$	η	$\Delta\eta$	η	$\Delta\eta$	η	$\Delta\eta$	η	$\Delta\eta$
x_1	mPa·s	mPa·s	mPa·s	mPa·s	mPa·s	mPa·s	mPa·s	mPa·s	mPa·s	mPa·s	mPa·s	mPa·s	mPa·s	mPa·s
($[\text{Im}][\text{C}_7\text{CO}_2]$ + Water)														
0	1.002	0	0.890	0	0.797	0	0.718	0	0.651	0	0.587	0	0.556	0
0.1846	20.63	-3.48	17.59	-3.71	14.75	-3.68	12.62	-3.67	10.93	-3.59	9.916	-3.80	9.303	-4.17
0.2005	22.18	-3.64	18.69	-3.69	16.00	-4.04	13.52	-3.87	11.72	-3.80	10.40	-3.81	9.764	-4.24
0.3357	34.90	-4.53	29.09	-4.57	24.26	-4.77	20.32	-4.64	17.17	-4.34	14.90	-4.25	13.40	-4.53
0.3983	39.83	-3.99	32.99	-4.07	27.23	-4.26	22.30	-3.82	18.94	-3.85	16.16	-3.63	14.35	-3.93
0.4881	45.74	-2.04	37.40	-2.16	30.40	-2.42	25.00	-2.52	20.82	-2.47	17.87	-2.65	15.72	-3.07
0.5909	50.43	2.26	41.10	1.38	33.00	0.70	26.50	0.56	21.89	0.19	18.60	-0.30	16.17	-0.97
0.6958	53.53	8.34	43.30	6.56	34.60	4.94	27.60	4.14	22.80	3.09	19.22	2.23	16.85	0.94
0.8036	58.59	12.71	46.30	11.1	36.57	8.98	29.22	7.32	24.17	5.63	20.39	4.28	17.55	2.92
0.9011	67.90	11.93	54.06	10.2	41.70	9.28	33.19	7.70	27.32	6.01	23.17	4.43	19.77	3.11
1	88.48	0	71.27	0	56.48	0	45.30	0	36.92	0	30.56	0	25.33	0
($[\text{Im}][\text{C}_7\text{CO}_2]$ + Acetonitrile)														
0	0.350	0	0.3330	0	0.325	0	0.292	0	0.279	0	0.245	0	0.223	0
0.1004	1.201	-7.76	1.199	-6.20	1.210	-4.71	1.241	-3.56	1.397	-2.58	1.770	-1.58	1.600	-1.25
0.3076	5.800	-20.93	6.300	-15.68	5.600	-11.85	5.500	-8.60	4.400	-7.19	5.100	-4.65	5.376	-2.91
0.4005	10.60	-24.09	10.00	-18.52	9.600	-13.02	8.400	-9.87	7.398	-7.91	7.511	-4.83	7.600	-2.87
0.5010	17.94	-25.38	16.11	-19.49	14.67	-13.55	12.80	-9.98	11.40	-7.31	10.70	-5.03	10.20	-2.83
0.5995	25.96	-25.80	22.70	-19.83	20.17	-13.53	17.89	-9.31	15.60	-6.73	14.10	-4.68	13.20	-2.33
0.7020	37.82	-22.73	32.00	-17.75	27.47	-11.94	23.68	-8.80	20.83	-5.27	18.21	-3.74	16.21	-1.93
0.8014	50.42	-18.66	41.88	-14.87	35.30	-9.64	30.04	-6.56	26.10	-3.65	22.30	-2.72	19.55	-1.36
0.8956	66.00	-11.16	54.30	-9.08	45.40	-4.79	37.00	-3.49	31.40	-1.82	26.31	-1.36	22.52	-0.27
1	88.48	0	71.27	0	56.48	0	45.30	0	36.92	0	30.56	0	25.33	0
($[\text{Im}][\text{C}_7\text{CO}_2]$ + Ethanol)														
0	1.21	0	1.100	0	1.000	0	0.910	0	0.830	0	0.720	0	0.615	0
0.1011	3.236	6.77	2.949	5.25	2.686	3.92	2.471	2.93	2.278	2.20	2.125	1.61	1.600	1.13
0.2001	6.029	12.63	5.466	9.68	4.927	7.18	4.540	5.25	4.194	3.86	3.962	2.73	4.433	1.13
0.2994	10.32	17.00	9.322	12.79	8.398	9.21	7.772	6.43	6.900	4.74	6.300	3.35	6.400	1.62
0.4001	14.5	21.61	13.30	15.88	12.00	11.20	11.40	7.27	9.900	5.37	9.000	3.66	8.900	1.60
0.5214	22.9	23.80	20.00	17.69	17.80	12.13	16.40	7.65	14.00	5.65	12.60	3.68	12.00	1.50
0.6000	29.8	23.76	25.50	17.70	22.30	11.99	19.90	7.64	17.20	5.28	15.30	3.32	14.10	1.34
0.6990	40.4	21.80	34.00	16.15	28.90	10.88	24.80	7.14	21.50	4.56	18.80	2.78	16.70	1.19
0.8016	53.79	17.37	44.47	12.88	36.53	8.94	30.43	6.06	26.09	3.67	22.40	2.24	19.60	0.83
0.8957	68.68	10.69	55.78	8.17	44.96	5.73	36.81	3.86	31.00	2.16	26.20	1.25	22.30	0.45
1	88.48	0	71.27	0	56.48	0	45.30	0	36.92	0	30.56	0	25.33	0
($[\text{Im}][\text{C}_7\text{CO}_2]$ + 1-Octanol)														
0	9.183	0	7.840	0	6.420	0	5.341	0	4.661	0	3.701	0	2.840	0
0.1003	10.50	-6.63	9.100	-4.69	8.330	-3.11	7.641	-2.25	5.937	-1.61	5.377	-1.02	4.821	0.86
0.2010	13.40	-11.72	11.70	-8.52	10.00	-6.48	9.401	-3.97	7.500	-3.15	6.700	-2.40	5.900	-0.50
0.3001	18.00	-14.98	15.39	-11.17	13.24	-8.20	11.72	-5.61	9.786	-4.56	8.459	-3.30	7.480	-1.44
0.3995	24.00	-16.86	20.30	-12.60	17.20	-9.22	14.95	-6.36	12.30	-5.25	10.70	-3.73	9.400	-2.42
0.4993	30.85	-17.93	25.90	-13.38	21.67	-9.74	18.76	-6.53	15.57	-5.20	13.05	-4.06	11.60	-2.47
0.6000	39.42	-17.34	33.30	-12.42	27.50	-8.96	23.23	-6.08	19.40	-4.62	16.40	-3.42	14.21	-2.12
0.7009	51.03	-13.73	41.90	-10.26	34.44	-7.07	28.56	-4.79	23.44	-3.83	19.80	-2.73	17.10	-1.50
0.8001	64.44	-8.19	52.31	-6.19	42.20	-4.27	34.63	-2.68	28.50	-1.97	23.63	-1.56	20.17	-0.66
0.8989	78.05	-2.41	63.19	-1.62	50.26	-1.15	40.69	-0.56	33.14	-0.52	27.68	-0.41	22.90	-0.15
1	88.48	0	71.27	0	56.48	0	45.30	0	36.92	0	30.56	0	25.33	0

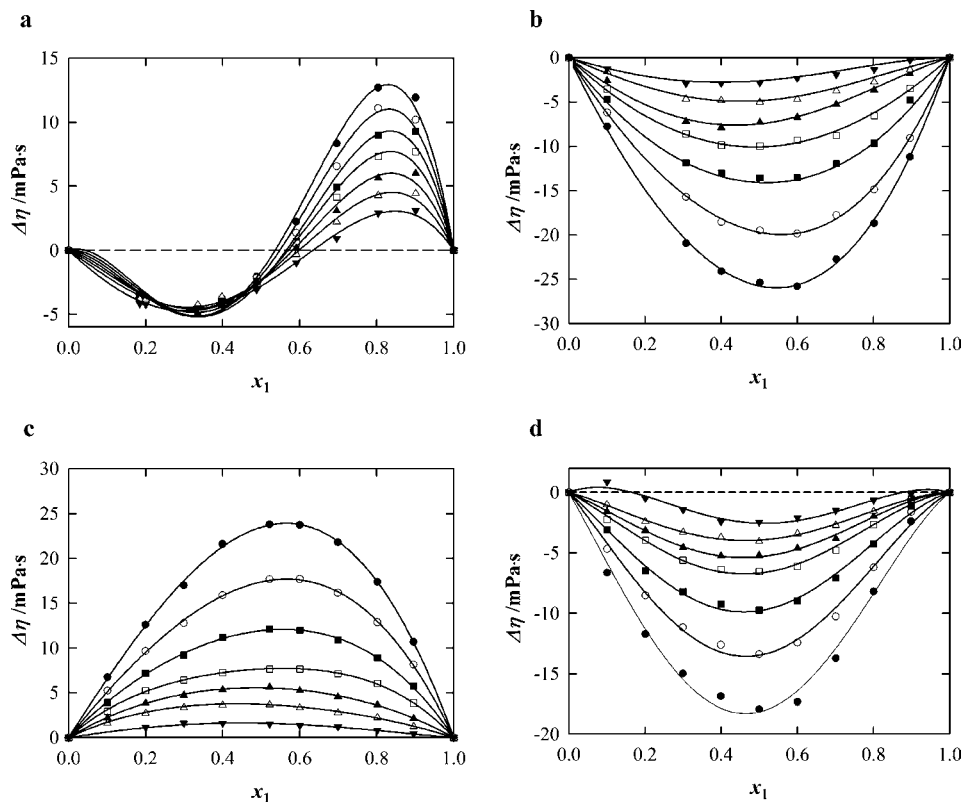


Figure 5. Comparison of viscosity deviations from ideality, $\Delta\eta$, against mole fraction of $[\text{Im}][\text{C}_7\text{CO}_2]$, x_1 , for: a, ($[\text{Im}][\text{C}_7\text{CO}_2]$ + water); b, ($[\text{Im}][\text{C}_7\text{CO}_2]$ + acetonitrile); c, ($[\text{Im}][\text{C}_7\text{CO}_2]$ + ethanol); d, ($[\text{Im}][\text{C}_7\text{CO}_2]$ + 1-octanol); mixtures as a function of the temperature T : \circ , 293.15 K; \bullet , 298.15 K; \square , 303.15 K; \blacksquare , 308.15 K; \blacktriangle , 313.15 K; \triangle , 318.15 K; \blacktriangledown , 323.15 K. The lines represent the Redlich–Kister-type fittings using three adjustable parameters.

(or $\bar{V}_{m,i}$) to $x_i = 0$ at 298.15 K for each investigated systems. From Figure 2, $\bar{V}_{m,1}$ values have the following order: 1-octanol > water > ethanol > acetonitrile. This sequence may indicate that acetonitrile interacts more strongly with the $[\text{Im}][\text{C}_7\text{CO}_2]$ than other studied molecular solvents.

Viscosities of ($[\text{Im}][\text{C}_7\text{CO}_2]$ + Solvent) Binary Mixtures and Temperature Effect. Since ILs are more viscous than conventional solvents, in most applications, they can be used in mixtures with other less viscous fluids. Therefore, the viscosity of pure ILs and their mixtures with conventional solvents is an important property, and their knowledge is primordial for each industrial processes. The viscosity of the pure imidazolium octanoate is studied from (293.15 to 323.15) K and reported herein in Figure 3. The viscosity of pure $[\text{Im}][\text{C}_7\text{CO}_2]$ decreases with the temperature from (88.48 to 25.33) mPa·s at (293.15 and 333.15) K, respectively. Experimental values were then adjusted by using the conventional Vogel–Tammann–Fulcher (VTF) equation according to the following equation:

$$\eta = \eta_0 \exp\left[\frac{B}{T - T_0}\right] \quad (6)$$

where η_0 , B , and T_0 are constants. The best-fit parameters for the pure PIL viscosity is obtained for $\eta_0 = 0.0108$ mPa·s, $B = 1680$ K, and $T_0 = 106.8$ K, giving an percent relative absolute deviation (RAD) close to 0.64 % as visualized in the Figure 3.

The temperature effect on the viscosity of each investigated ($[\text{Im}][\text{C}_7\text{CO}_2]$ + solvent) binary system was measured by increasing and then decreasing the temperature from (293.15 to 363.15) K. Figure 4 reports an example of this temperature effect in the case of the ($[\text{Im}][\text{C}_7\text{CO}_2]$ + 1-octanol) binary

mixture for an $[\text{Im}][\text{C}_7\text{CO}_2]$ mole fraction, $x_1 = 0.2$, and Figure S5 for four other mole fractions ($x_1 = 0.1$ (a); 0.3 (b); 0.5 (c); 0.7 (d)) in the Supporting Information. We show that the viscosity variation against temperature presents a hysteresis with a minimum at $T = 335$ K. This behavior, also observed with water, acetonitrile, and ethanol solutions, can be explained by a micelle formation in the (PIL + 1-octanol) mixture. The micelle formation for $[\text{Im}][\text{C}_7\text{CO}_2]$, already described in previously work,³⁵ is favored by increasing the temperature and could explain that the viscosity increases by increasing the temperature from $T = (330 \text{ to } 370)$ K as shown in Figure 4. By then cooling the solution, the viscosity of the micellar system decreases lesser than the viscosity of nonmicellar solution, until reobtaining similar viscosity values for temperatures below 310 K. In other words, this temperature effect was not caused by a composition change within the temperature, but by most-probably a micellar formation between $[\text{Im}][\text{C}_7\text{CO}_2]$ and 1-octanol. A similar temperature effect was observed for binary systems containing water, acetonitrile, and ethanol in the whole composition range.

The viscosity deviations $\Delta\eta$ were calculated from the eq 7:

$$\Delta\eta = \eta - (x_1\eta_1 + x_2\eta_2) \quad (7)$$

where x_1 and x_2 are the mole fractions of $[\text{Im}][\text{C}_7\text{CO}_2]$ and solvent, η , η_1 , and η_2 are the viscosity of the solution, the pure PIL, and the pure solvent, respectively. Experimental data of the viscosities η and viscosity deviation $\Delta\eta$ are listed in Table 3.

Figure S4a–d of the Supporting Information and Figure 5a–d show the dependence of the viscosity and viscosity deviations from ideality $\Delta\eta$, against the mole fraction of $[\text{Im}][\text{C}_7\text{CO}_2]$, x_1 , and temperature T from (298.15 to 323.15) K in the case of

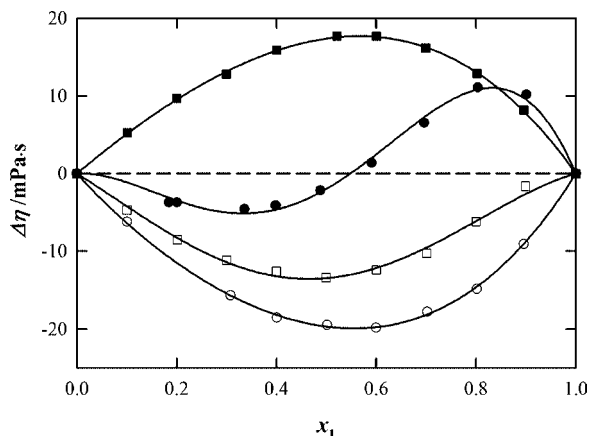


Figure 6. Comparison of viscosity deviations from ideality, $\Delta\eta$, against the mole fraction of $[\text{Im}][\text{C}_7\text{CO}_2]$, x_1 , for $([\text{Im}][\text{C}_7\text{CO}_2] + \text{molecular solvent})$ at 298.15 K: ●, water; ○, acetonitrile; ■, ethanol; □, 1-octanol. The lines represent the Redlich–Kister-type fittings with the parameters indicated in Table 1.

$([\text{Im}][\text{C}_7\text{CO}_2] + \text{water})$ (a), $([\text{Im}][\text{C}_7\text{CO}_2] + \text{acetonitrile})$ (b), $([\text{Im}][\text{C}_7\text{CO}_2] + \text{ethanol})$ (c), and $([\text{Im}][\text{C}_7\text{CO}_2] + 1\text{-octanol})$ (d) binary mixtures, respectively. It can be seen in Table 3 and Figure 5c that in the case of ethanol, for all temperatures studied, $\Delta\eta$ is symmetrically positive over the entire composition range and decreases with increasing temperature, whereas, for 1-octanol and acetonitrile, $\Delta\eta$ of the $([\text{Im}][\text{C}_7\text{CO}_2] + \text{solvent})$ binary mixtures presents a symmetrical negative deviation in the whole mole fraction range and becomes less negative with increasing temperature (Table 3 and Figures 5b and 9d). In the case of $([\text{Im}][\text{C}_7\text{CO}_2] + \text{water})$ binary mixtures, $\Delta\eta$ presents an S-shape with negative deviations for $x_1 < 0.5$ and positive deviations for $x_1 > 0.5$. The maximum of the deviation $\Delta\eta$ is observed at $x_1 = 0.8$. In fact, the temperature influences strongly the viscosity deviations, but the observed compositions at the maximum in viscosity deviations were found to be almost constant and independent of temperature in each case.

In Figure 6, we report, for comparison, the viscosity deviations as a function of PIL mole fraction, x_1 , at 298.15 K for all studied $([\text{Im}][\text{C}_7\text{CO}_2] + \text{solvent})$ binary mixtures. It can be seen that the absolute deviation values, $|\Delta\eta|$, are from (5 to 20) $\text{mPa}\cdot\text{s}$. Furthermore, the viscosity deviations show extrema near to equimolar compositions region ($x_1 < 0.5$) in the case of alcohols and acetonitrile solutions, and maxima were localized, in the case of water solutions, in the IL-rich composition region.

According to Bearman and Jones,⁴⁰ the viscosity of a mixture depends strongly on its entropy, which is related with the liquid's

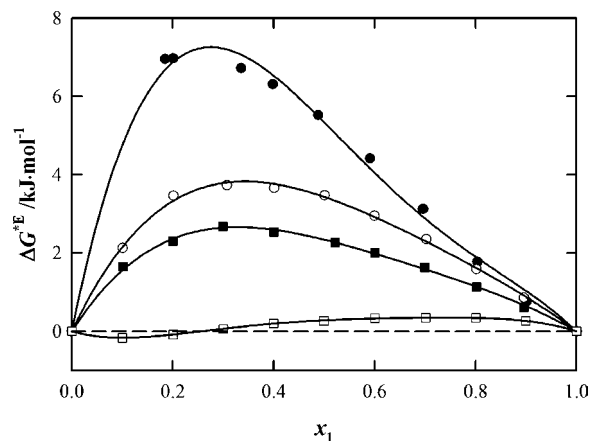


Figure 7. Comparison of the excess Gibbs free energy of activation of viscous flow, ΔG^{*E} , for binary mixtures of $([\text{Im}][\text{C}_7\text{CO}_2] + \text{molecular solvent})$ at 298.15 K as a function of $[\text{Im}][\text{C}_7\text{CO}_2]$ mole fraction composition, x_1 : ●, water; ○, acetonitrile; ■, ethanol; □, 1-octanol. The lines are just a guide to the eye.

structure. Therefore, the viscosity deviation depends on molecular interactions as well as on the size and shape of the molecules. It can be seen in Figure 6 that, for acetonitrile and 1-octanol, the viscosity deviations are negative over the whole composition range. This behavior is characteristic of mixtures without strong specific interactions. On the contrary, $([\text{Im}][\text{C}_7\text{CO}_2] + \text{ethanol})$ and $([\text{Im}][\text{C}_7\text{CO}_2] + \text{water})$ mixtures exhibit positive and S-shape deviations with the mole fraction compositions, respectively. These viscosity variations could be attributed to the break-up of the self-association through hydrogen bonding. The sign of $\Delta\eta$ deviation can be explained by the competition between H-bonds and van der Waals interactions present in mixtures containing a molecular solvent and an ionic species. In the case of the mixture dominated by the van der Waals interactions (such as mixtures containing acetonitrile or 1-octanol), the $\Delta\eta$ deviation is negative. On the contrary, for mixtures containing ethanol, which is a protic solvent dominated by an H-bond, $\Delta\eta$ is positive. In the case of water, which presents strong H-bonds and van der Waals interactions, the sign of $\Delta\eta$ deviation depends on the composition, in other words, of the intermolecular association between the solute and the solvent.

On the basis of the theory of absolute reaction rates,⁴¹ the excess Gibbs energies (ΔG^{*E}) of activation of viscous flow were calculated from eq 8:

Table 4. Excess Gibbs Free Energy of Activation of Viscous Flow, ΔG^{*E} , for Binary Mixtures of $\{[\text{Im}][\text{C}_7\text{CO}_2] + \text{Molecular Solvent}\}$ at 298.15 K as a Function of $[\text{Im}][\text{C}_7\text{CO}_2]$ Mole Fraction Composition, x_1^a

($[\text{Im}][\text{C}_7\text{CO}_2] + \text{water}$)		($[\text{Im}][\text{C}_7\text{CO}_2] + \text{acetonitrile}$)		($[\text{Im}][\text{C}_7\text{CO}_2] + \text{ethanol}$)		($[\text{Im}][\text{C}_7\text{CO}_2] + 1\text{-octanol}$)	
ΔG^{*E}		ΔG^{*E}		ΔG^{*E}		ΔG^{*E}	
x_1	$\text{kJ}\cdot\text{mol}^{-1}$	x_1	$\text{kJ}\cdot\text{mol}^{-1}$	x_1	$\text{kJ}\cdot\text{mol}^{-1}$	x_1	$\text{kJ}\cdot\text{mol}^{-1}$
0	0	0	0	0	0	0	0
0.1846	6.95	0.1004	2.12	0.1011	1.65	0.1003	-0.16
0.2005	6.97	0.2012	3.46	0.2001	2.30	0.2010	-0.08
0.3357	6.72	0.3076	3.73	0.2994	2.67	0.3001	0.06
0.3983	6.31	0.4005	3.65	0.4001	2.53	0.3995	0.20
0.4881	5.52	0.5010	3.47	0.5214	2.26	0.4993	0.26
0.5909	4.41	0.5995	2.95	0.6000	2.01	0.6000	0.33
0.6958	3.12	0.7020	2.34	0.6990	1.62	0.7009	0.34
0.8036	1.77	0.8014	1.58	0.8016	1.13	0.8001	0.34
0.9011	0.75	0.8956	0.85	0.8957	0.61	0.8989	0.26
1	0	1	0	1	0	1	0

^a The AAD for ΔG^{*E} is 2 %.

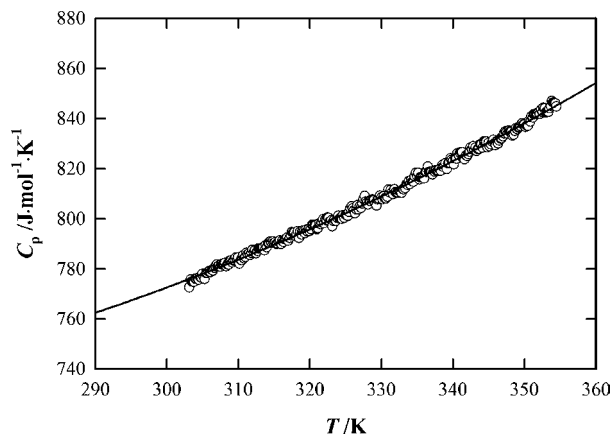


Figure 8. Molar heat capacities, C_p , of pure $[\text{Im}][\text{C}_7\text{CO}_2]$ as a function of the temperature. The line represents a polynomial-type fitting with parameters reported in eq 9.

$$\frac{\Delta G^{*E}}{RT} = \left[\ln\left(\frac{\eta V}{\eta_2 V_{m,2}}\right) - x_1 \ln\left(\frac{\eta_1 V_{m,1}}{\eta_2 V_{m,2}}\right) \right] \quad (8)$$

where V , $V_{m,1}$, and $V_{m,2}$ are the molar volumes of the binary mixture and pure components. Calculated values of ΔG^{*E} are shown in Table 4. The ΔG^{*E} for the binary mixtures are positive as shown in Figure 7, and ΔG^{*E} values steadily increases with the PIL mole fraction up close to 0.2. The observed ΔG^{*E} values

are positive for the entire mole fraction of ($[\text{Im}][\text{C}_7\text{CO}_2]$ + molecular solvent) binary systems, except in the case of 1-octanol mixture, which described an S-shape of ΔG^{*E} values as a function of composition with a lower amplitude. Large positive values (in the case of water and acetonitrile binary mixtures) indicate the specific interaction leading to complex formation through intermolecular hydrogen bonding or van der Waals interaction between unlike molecules compared to like molecules.⁴²

Study of the Heat Capacities for ($[\text{Im}][\text{C}_7\text{CO}_2]$ + Molecular Solvent) Binary Systems. The specific heat capacities at constant pressure of the pure $[\text{Im}][\text{C}_7\text{CO}_2]$ were obtained from (303.15 to 353.15) K (Figure 8). The specific heat capacities of pure $[\text{Im}][\text{C}_7\text{CO}_2]$ increase with temperature and were fitted according to the following equations:

$$C_p = 747.7 + 7.9 \cdot 10^{-1}(T) + 5.10 \cdot 10^{-3}(T)^2 \quad (9)$$

The specific heat capacities of ($[\text{Im}][\text{C}_7\text{CO}_2]$ + molecular solvent) systems, C_p , were then determined at various temperatures from (298.15 to 313.15) K, and obtained values are listed in Table 5. The excess heat capacities, C_p^E , of the ($[\text{Im}][\text{C}_7\text{CO}_2]$ + molecular solvent) binary systems were calculated using the following relationship:

Table 5. Molar Heat Capacities, C_p , and Excess Molar Heat Capacities, C_p^E , for ($[\text{Im}][\text{C}_7\text{CO}_2]$ + Molecular Solvent) as a Function of $[\text{Im}][\text{C}_7\text{CO}_2]$ Mole Fraction Composition, x_1 , and Temperature up to 313.15 K

T/K	298.15		303.15		308.15		313.15	
	C_p	C_p^E	C_p	C_p^E	C_p	C_p^E	C_p	C_p^E
x_1	$\text{J}\cdot\text{mol}^{-1}\cdot\text{K}^{-1}$	$\text{J}\cdot\text{mol}^{-1}\cdot\text{K}^{-1}$	$\text{J}\cdot\text{mol}^{-1}\cdot\text{K}^{-1}$	$\text{J}\cdot\text{mol}^{-1}\cdot\text{K}^{-1}$	$\text{J}\cdot\text{mol}^{-1}\cdot\text{K}^{-1}$	$\text{J}\cdot\text{mol}^{-1}\cdot\text{K}^{-1}$	$\text{J}\cdot\text{mol}^{-1}\cdot\text{K}^{-1}$	$\text{J}\cdot\text{mol}^{-1}\cdot\text{K}^{-1}$
($[\text{Im}][\text{C}_7\text{CO}_2]$ + Acetonitrile)								
0	91.69	0	92.21	0	92.40	0	92.82	0
0.1004	137.6	-22.1	154.1	-6.41	173.2	11.6	183.8	21.2
0.2012	215.8	-12.1	248.1	19.0	280.7	49.6	307.4	74.7
0.3076	337.2	37.2	395.8	94.4	430.2	126	457.1	150
0.4005	499.6	137	544.0	179	574.1	206	609.0	238
0.5010	675.7	245	725.8	293	751.8	314	791.1	350
0.5995	845.9	348	890.8	391	924.9	419	979.9	470
0.7020	995.6	428	1047	477	1083	506	1120	539
0.8014	1046	411	1100	463	1149	504	1185	535
0.8956	1020	322	1045	343	1052	342	1054	339
1	769.0	0	772.4	0	782.2	0	788.1	0
($[\text{Im}][\text{C}_7\text{CO}_2]$ + Ethanol)								
0	112.0	0	114.0	0	116.0	0	118.0	0
0.1011	188.6	10.1	187.3	6.74	187.1	3.78	186.6	0.811
0.2001	256.6	13.1	255.1	9.32	254.3	4.91	253.8	1.65
0.2994	317.3	8.54	315.6	4.36	312.3	-3.21	308.3	-10.4
0.4001	364.9	-10.0	360.4	-17.1	358.7	-23.9	357.0	-29.1
0.5214	420.0	-34.6	419.9	-37.5	421.1	-42.3	419.7	-47.8
0.6000	458.2	-48.0	459.4	-49.7	462.5	-53.3	464.1	-56.1
0.6990	516.2	-55.0	517.1	-57.2	520.9	-60.8	523.8	-62.7
0.8016	591.0	-47.6	591.6	-50.4	596.5	-53.7	599.4	-55.8
0.8957	667.5	-32.9	673.1	-30.7	681.9	-30.9	683.6	-34.7
1	769.0	0	772.6	0	782.3	0	788.2	0
($[\text{Im}][\text{C}_7\text{CO}_2]$ + 1-Octanol)								
0	304.0	0	329.0	0	354.0	0	379.0	0
0.1003	469.0	118	479.0	106.0	483.0	86.1	497.0	77.0
0.2010	570.9	173	566.2	148.0	556.1	116.0	561.1	100.1
0.3001	603.8	160	601.4	139.0	598.1	116.0	592.2	90.4
0.3995	591.7	102	599.3	93.1	613.1	88.0	606.7	64.2
0.4993	571.6	35.4	579.9	29.4	594.4	26.5	604.1	20.8
0.6000	547.5	-35.5	565.6	-29.6	587.6	-23.4	596.3	-28.3
0.7009	540.4	-89.5	534.5	-105	585.6	-68.6	607.0	-58.8
0.8001	534.8	-141	557.8	-126	605.7	-91.0	633.3	-73.1
0.8989	606.3	-116	638.3	-89.4	656.8	-82.2	681.9	-64.9
1	769.0	0	772.6	0	782.3	0	788.2	0

$$C_p^E = C_p - (x_1 C_{p1}^0 + x_2 C_{p2}^0) \quad (10)$$

where C_{p1}^0 and C_{p2}^0 denote the heat capacities of pure compounds and x_1 and x_2 are their mole fractions, respectively. Calculated excess specific heat capacities C_p^E are reported at each temperature in Table 5.

Figure 9a–c shows the dependence of the excess specific heat capacities C_p^E against the mole fraction of [Im][C₇CO₂], x_1 , and temperature T from (298.15 to 313.15) K in the case of ([Im][C₇CO₂] + acetonitrile) (a), ([Im][C₇CO₂] + ethanol) (b), and ([Im][C₇CO₂] + 1-octanol) (c) binary mixtures, respectively. Figure 10 shows the comparison of excess molar heat capacities of binary mixtures of ([Im][C₇CO₂] + molecular solvent) at 298.15 K as a function of [Im][C₇CO₂] mole fraction composition, x_1 . For all studied mixtures, C_p^E describe S-shapes with the composition, while for acetonitrile mixtures, the C_p^E deviation is strongly positive for the IL-rich composition ($C_p^E \approx 430 \text{ J}\cdot\text{mol}^{-1}\cdot\text{K}^{-1}$ at $x_1 = 0.70$). For the mixtures with alcohols, maxima of positive and negative deviations were obtained for $x_1 = 0.2$ and 0.8 , respectively. C_p^E of binary mixtures with 1-octanol ($C_p^E \approx 170 \text{ J}\cdot\text{mol}^{-1}\cdot\text{K}^{-1}$ at $x_1 = 0.2$) are higher than values obtained with ethanol ($C_p^E \approx 13 \text{ J}\cdot\text{mol}^{-1}\cdot\text{K}^{-1}$ at $x_1 = 0.2$).

The dependence of the excess molar heat capacity on the mixture composition reflects indirectly the interactions between molecules in solution^{17,43} and can be showed by the example of ethanol mixtures of PIL (Figure 9b). The negative values C_p^E for binary mixtures containing a protic solvent like ethanol and a proton donor like an imidazolium cation and a proton acceptor like a carboxylate anion can be interpreted as result of two competing processes: self-association of ethanol molecules or PIL molecules at infinite dilution of PIL or ethanol in the mixture and heteromolecular association through hydrogen

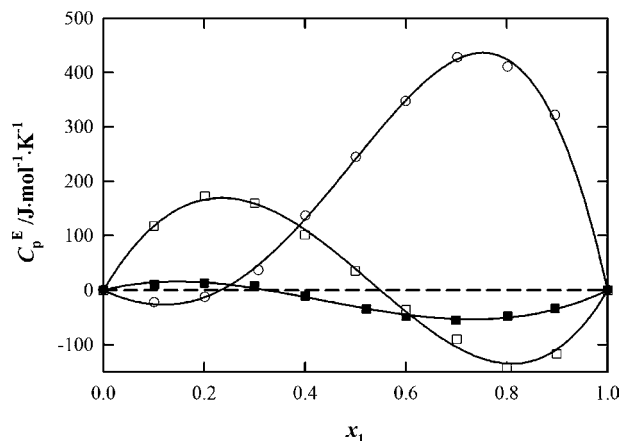


Figure 10. Comparison of excess molar heat capacities of binary mixtures of ([Im][C₇CO₂] + molecular solvent) at 298.15 K as a function of [Im][C₇CO₂] mole fraction composition, x_1 : ○, acetonitrile; ■, ethanol; □, 1-octanol. The lines represent the Redlich–Kister-type fittings with the parameters indicated in the Table 1.

bonds. The first addition of PIL to ethanol has a drastic effect on the structure of ethanol: ions from the PIL are structure-breaking for the hydrogen bonds in ethanol. For acetonitrile the inverse effect is observed, and heteromolecule associations between CH₃CN and [Im][C₇CO₂] give rise to a positive contribution to C_p^E .¹⁸ In the case of 1-octanol, the strong interaction of the long alkyl chain length of the alcohol is added to the interaction, between the anion group –CO₂[−] and the imidazolium cation, arising from the heteromolecular association through hydrogen bonds.

Redlich–Kister Equations. V^E , C_p^E , and $\Delta\eta$ values for the ([Im][C₇CO₂] + solvent) systems as a function of composition

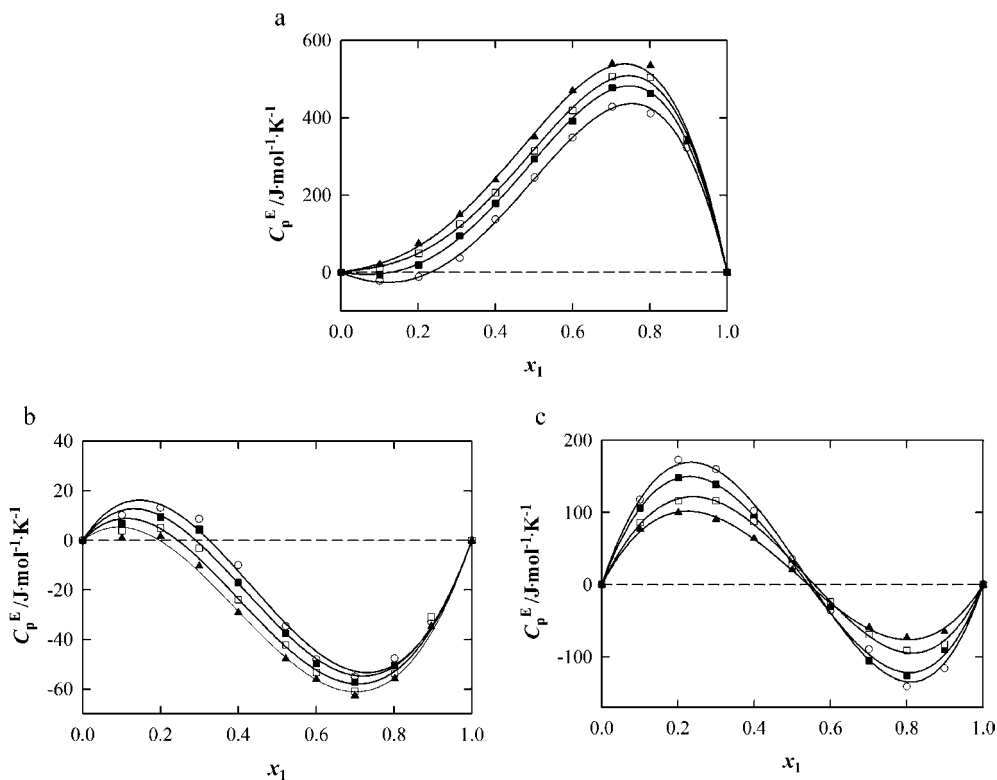


Figure 9. Comparison of excess molar heat capacities, C_p^E , against the mole fraction of [Im][C₇CO₂], x_1 , for: a, ([Im][C₇CO₂] + acetonitrile); b, ([Im][C₇CO₂] + ethanol); c, ([Im][C₇CO₂] + 1-octanol); mixtures as a function of the temperature T : ○, 298.15 K; ■, 303.15 K; □, 308.15 K; ▼, 313.15 K. The lines represent the Redlich–Kister-type fittings using three adjustable parameters.

Table 6. Redlich–Kister Fitting Coefficients A_i and the Average of the RADs of the Excess Molar Volumes, V^E , and Excess Molar Heat Capacities, C_p^E , for the Binary Mixtures of ([Im][C₇CO₂] + Molecular Solvent) as a Function of [Im][C₇CO₂] Mole Fraction Composition, x_1 , at 298.15 K

Y^E	molecular solvent	A_0	A_1	A_2	100·RAD
V^E (cm ³ ·mol ⁻¹)	water	-2.8059	+2.5205	-1.3483	3.4
	acetonitrile	-7.5604	-4.3981	-5.8826	2.6
	ethanol	-4.0833	2.1386	1.5313	6.4
	1-octanol	2.0143	-1.423	-1.0394	6.0
C_p^E (J·mol ⁻¹ ·K ⁻¹)	acetonitrile	+963.9	+2279	+895	6.6
	ethanol	-119.9	-337.1	+20.64	11
	1-octanol	+156.7	-1566	-156.0	7.2
	water	-7.8666	+74.078	+85.310	16
$\Delta\eta$ (mPa·s)	water	-7.8666	+74.078	+85.310	16
	acetonitrile	-78.735	-16.425	-7.9515	1.2
	ethanol	+69.508	+18.441	+3.1136	1.2
	1-octanol	-53.869	+11.058	+24.998	10

and temperature were fitted by using the Redlich–Kister-type polynomial equation.⁴⁴

$$Y^E = x_1 x_2 \sum_{i=0}^m A_i (1 - 2x_2)^i \quad (11)$$

where Y^E represents V^E , C_p^E , and $\Delta\eta$, x_1 and x_2 are the mole fraction of the components 1 and 2, and A_i are the adjustable parameters. The optimum number of adjustable parameters A_i was ascertained from an examination of the RAD, and the results are reported in Table 6.

Conclusion

Volumetric properties of ([Im][C₇CO₂] + solvent) binary systems with four molecular solvents (water, ethanol, 1-octanol, and acetonitrile) were studied at 298.15 K. Different behaviors were observed which reflected differences in the volumetric properties of the (PIL + solvent) systems. The volume excess, V^E , for solutions of imidazolium octanoate, [Im][C₇CO₂], and molecular solvents were determined from the experimental data. They exhibit negative deviations from the ideal behavior over the entire range for all (PIL + solvent) systems except in the case of 1-octanol. The apparent molar volumes at infinite dilution (partial molar volume at infinite dilution) for [Im][C₇CO₂] in all solvents have been then obtained. Viscosities and their deviation from ideality rules, $\Delta\eta$, are studied as a function of composition and temperature for the four studied systems. On the basis of the theory of absolute reaction rates, the excess Gibbs energies (ΔG^{*E}) of activation of viscous flow are calculated. The observed ΔG^{*E} values are positive for the entire mole fraction ([Im][C₇CO₂] + molecular solvent), except in the case of the 1-octanol mixture, which describes an S-shape of ΔG^{*E} values as a function of composition. Large positive values for water and acetonitrile mixtures indicate the specific interaction leading to complex formation through intermolecular hydrogen bonding. The dependence of the excess molar heat capacity, C_p^E , on the mixture composition reflects indirectly the interactions between molecules in solution and can be shown by the different behavior of the deviation of C_p^E according to the nature of the solvent in PIL solution. Finally, excess properties were, then, fitted to the Redlich–Kister polynomial equation.

Acknowledgment

Thanks to Perrine Parrotot for their precious help for some experimental measures.

Supporting Information Available:

Additional information of the PIL characterization and ([Im][C₇CO₂] + molecular solvent) binary systems. This material is available free of charge via the Internet at <http://pubs.acs.org>.

Literature Cited

- Crosthwaite, J. M.; Aki, S.; Maginn, E. J.; Brennecke, J. F. Liquid phase behavior of imidazolium-based ionic liquids with alcohols. *J. Phys. Chem. B* **2004**, *108*, 5113–5119.
- Earle, M. J.; Esperanca, J.; Gilea, M. A.; Lopes, J. N. C.; Rebelo, L. P. N.; Magee, J. W.; Seddon, K. R.; Widegren, J. A. The distillation and volatility of ionic liquids. *Nature* **2006**, *439*, 831–834.
- Kumar, A. Estimates of internal pressure and molar refraction of imidazolium based ionic liquids as a function of temperature. *J. Solution Chem.* **2008**, *37*, 203–214.
- Tokuda, H.; Tsuzuki, S.; Susan, M.; Hayamizu, K.; Watanabe, M. How ionic are room-temperature ionic liquids? An indicator of the physicochemical properties. *J. Phys. Chem. B* **2006**, *110*, 19593–19600.
- Welton, T. Room-temperature ionic liquids. Solvents for synthesis and catalysis. *Chem. Rev.* **1999**, *99*, 2071–2083.
- Wilkes, J. S. Properties of ionic liquid solvents for catalysis. *J. Mol. Catal. A: Chem.* **2004**, *214*, 11–17.
- Greaves, T. L.; Drummond, C. J. Protic ionic liquids: Properties and applications. *Chem. Rev.* **2008**, *108*, 206–237.
- Araos, M. U.; Warr, G. G. Self-assembly of nonionic surfactants into lyotropic liquid crystals in ethylammonium nitrate, a room-temperature ionic liquid. *J. Phys. Chem. B* **2005**, *109*, 14275–14277.
- Evans, D. F. Self-organization of amphiphiles. *Langmuir* **1988**, *4*, 3–12.
- Greaves, T. L.; Weerawardena, A.; Fong, C.; Drummond, C. J. Formation of amphiphile self-assembly phases in protic ionic liquids. *J. Phys. Chem. B* **2007**, *111*, 4082–4088.
- Greaves, T. L.; Weerawardena, A.; Fong, C.; Drummond, C. J. Many protic ionic liquids mediate hydrocarbon-solvent interactions and promote amphiphile self-assembly. *Langmuir* **2007**, *23*, 402–404.
- Spicer, P. T.; Small, W. B.; Lynch, M. L. Cubic liquid crystalline compositions and methods for their preparation. World Patent WO/2002/066014-A2, 2002.
- Janus, E.; Goc-Maciejewska, I.; Lozynski, M.; Pernak, J. Diels-Alder reaction in protic ionic liquids. *Tetrahedron Lett.* **2006**, *47*, 4079–4083.
- Lansalot-Matras, C.; Moreau, C. Dehydration of fructose into 5-hydroxymethylfurfural in the presence of ionic liquids. *Catal. Commun.* **2003**, *4*, 517–520.
- Zhao, G. Y.; Jiang, T.; Gao, H. X.; Han, B. X.; Huang, J.; Sun, D. H. Mannich reaction using acidic ionic liquids as catalysts and solvents. *Green Chem.* **2004**, *6*, 75–77.
- Angell, C. A.; Wang, L. M. Hyperquenching and cold equilibration strategies for the study of liquid-liquid and protein folding transitions. *Biophys. Chem.* **2003**, *105*, 621–637.
- Lau, R. M.; Sorgedraeger, M. J.; Carrea, G.; van Rantwijk, F.; Secundo, F.; Sheldon, R. A. Dissolution of *Candida antarctica* lipase B in ionic liquids: effects on structure and activity. *Green Chem.* **2004**, *6*, 483–487.
- Pernak, J.; Goc, I.; Fojutowski, A. Protic ionic liquids with organic anion as wood preservative. *Holzforschung* **2005**, *59*, 473–475.
- Angell, C. A.; Xu, W.; Belieres, J.-P.; Yoshizawa, M. Ionic liquids and ionic liquids acids with high temperature stability for fuel cell and other high temperature applications, method of making and cell employing same. World Patent WO/2004/114445, 2004.
- Noda, A.; Susan, A. B.; Kudo, K.; Mitsushima, S.; Hayamizu, K.; Watanabe, M. Bronsted acid-base ionic liquids as proton-conducting nonaqueous electrolytes. *J. Phys. Chem. B* **2003**, *107*, 4024–4033.
- Sun, J. Z.; Jordan, L. R.; Forsyth, M.; MacFarlane, D. R. Acid-organic base swollen polymer membranes. *Electrochim. Acta* **2001**, *46*, 1703–1708.
- Drake, G. W.; Hawkins, T. W.; Boatz, J.; Hall, L.; Vij, A. Experimental and theoretical study of 1,5-diamino-4-H-1,2,3,4-tetrazolium perchlorate. *Propellants, Explos., Pyrotech.* **2005**, *30*, 156–163.
- Gutowski, K. E.; Holbrey, J. D.; Rogers, R. D.; Dixon, D. A. Prediction of the formation and stabilities of energetic salts and ionic liquids based on ab initio electronic structure calculations. *J. Phys. Chem. B* **2005**, *109*, 23196–23208.
- Gardas, R. L.; Dagade, D. H.; Coutinho, J. A. P.; Patil, K. J. Thermodynamic studies of ionic interactions in aqueous solutions of imidazolium-based ionic liquids [Emim][Br] and [Bmim][Cl]. *J. Phys. Chem. B* **2008**, *112*, 3380–3389.
- Shekaari, H.; Mansoori, Y.; Sadeghi, R. Density, speed of sound, and electrical conductance of ionic liquid 1-hexyl-3-methyl-imidazolium bromide in water at different temperatures. *J. Chem. Thermodyn.* **2008**, *40*, 852–859.

- (26) Wang, J. J.; Wang, H. Y.; Zhang, S. L.; Zhang, H. H.; Zhao, Y. Conductivities, volumes, fluorescence, and aggregation behavior of ionic liquids [C(4)mim][BF₄] and [C(*n*)mim]Br (*n* = 4, 6, 8, 10, 12) in aqueous solutions. *J. Phys. Chem. B* **2007**, *111*, 6181–6188.
- (27) Domanska, U.; Pobudkowska, A.; Wisniewska, A. Solubility and excess molar properties of 1,3-dimethylimidazolium methylsulfate, or 1-butyl-3-methylimidazolium methylsulfate, or 1-butyl-3-methylimidazolium octylsulfate ionic liquids with *n*-alkanes and alcohols: Analysis in terms of the PFP and FBT models. *J. Solution Chem.* **2006**, *35*, 311–334.
- (28) Garcia-Miaja, G.; Troncoso, J.; Romani, L. Density and heat capacity as a function of temperature for binary mixtures of 1-butyl-3-methylpyridinium tetrafluoroborate plus water, plus ethanol, and plus nitromethane. *J. Chem. Eng. Data* **2007**, *52*, 2261–2265.
- (29) Liu, W. W.; Zhao, T. Y.; Zhang, Y. M.; Wang, H. P.; Yu, M. F. The physical properties of aqueous solutions of the ionic liquid [BMIM][BF₄]. *J. Solution Chem.* **2006**, *35*, 1337–1346.
- (30) Rebelo, L. P. N.; Najdanovic-Visak, V.; Visak, Z. P.; da Ponte, M. N.; Szydlowski, J.; Cerdeirina, C. A.; Troncoso, J.; Romani, L.; Esperanca, J.; Guedes, H. J. R.; de Sousa, H. C. A detailed thermodynamic analysis of [C(4)mim][BF₄] plus water as a case study to model ionic liquid aqueous solutions. *Green Chem.* **2004**, *6*, 369–381.
- (31) Zhang, Z. F.; Wu, W. Z.; Gao, H. X.; Han, B. X.; Wang, B.; Huang, Y. Tri-phase behavior of ionic liquid-water-CO₂ system at elevated pressures. *Phys. Chem. Chem. Phys.* **2004**, *6*, 5051–5055.
- (32) Wang, J. J.; Tian, Y.; Zhao, Y.; Zhuo, K. A volumetric and viscosity study for the mixtures of 1-*n*-butyl-3-methylimidazolium tetrafluoroborate ionic liquid with acetonitrile, dichloromethane, 2-butanone and *N,N*-dimethylformamide. *Green Chem.* **2003**, *5*, 618–622.
- (33) Wilkes, J. S. A short history of ionic liquids - from molten salts to neoteric solvents. *Green Chem.* **2002**, *4*, 73–80.
- (34) Diamond, R. M. Aqueous solution behavior of large univalent ions - A new type of ion pairing. *J. Phys. Chem.* **1963**, *67*, 2513–2517.
- (35) Anouti, M. J., Jr.; Boisset, A.; Jacquemin, J.; Caillon-Caravanier, M.; Lemordant, D. Aggregation behavior in water of new imidazolium and pyrrolidinium alkylcarboxylates protic ionic liquids. *J. Colloid Interface Sci.* **2009**, *340*, 104–111.
- (36) Crosthwaite, J. M.; Aki, S.; Maginn, E. J.; Brennecke, J. F. Liquid phase behavior of imidazolium-based ionic liquids with alcohols: effect of hydrogen bonding and non-polar interactions. *Fluid Phase Equilib.* **2005**, *228*, 303–309.
- (37) Najdanovic-Visak, V.; Esperanca, J.; Rebelo, L. P. N.; da Ponte, M. N.; Guedes, H. J. R.; Seddon, K. R.; de Sousa, H. C.; Szydlowski, J. Pressure, isotope, and water co-solvent effects in liquid-liquid equilibria of (ionic liquid plus alcohol) systems. *J. Phys. Chem. B* **2003**, *107*, 12797–12807.
- (38) Arce, A.; Rodil, E.; Soto, A. Physical and excess properties for binary mixtures of 1-methyl-3-octylimidazolium tetrafluoroborate, [Omim][BF₄], ionic liquid with different alcohols. *J. Solution Chem.* **2006**, *35*, 63–78.
- (39) Lachwa, J.; Morgado, P.; Esperanca, J.; Guedes, H. J. R.; Lopes, J. N. C.; Rebelo, L. P. N. Fluid-phase behavior of {1-hexyl-3-methylimidazolium bis(trifluoromethylsulfonyl) imide, [C(6)mim][NTf₂], plus C-2-C-8 *n*-alcohol} mixtures: Liquid-liquid equilibrium and excess volumes. *J. Chem. Eng. Data* **2006**, *51*, 2215–2221.
- (40) Bearman, R. J.; Jones, P. F. Statistical mechanical theory of the viscosity coefficients of binary liquid solutions. *J. Chem. Phys.* **1960**, *33*, 1432–1438.
- (41) Pal, A.; Kumar, H. Excess molar volumes and viscosities for binary liquid mixtures containing polyethers and pyrrolidin-2-one at 298.15 K. *Indian J. Chem., Sect. A: Inorg., Bioinorg., Phys., Theor. Anal. Chem.* **2001**, *40*, 598–604.
- (42) Kapadi, U. R.; Hundiwale, D. G.; Patil, N. B.; Lande, M. K.; Patil, P. R. Studies of viscosity and excess molar volume of binary mixtures of propane-1,2 diol with water at various temperatures. *Fluid Phase Equilib.* **2001**, *192*, 63–70.
- (43) Garlitz, J. A.; Summers, C. A.; Flowers, R. A.; Borgstahl, G. E. O. Ethylammonium nitrate: a protein crystallization reagent. *Acta Crystallogr., Sect. D: Biol. Crystallogr.* **1999**, *55*, 2037–2038.
- (44) De Oliveira, J. D. G.; Reis, J. C. R. The two faces of the Redlich-Kister equation and the limiting partial molar volume of water in 1-aminopropane-2-ol. *Thermochim. Acta* **2008**, *468*, 119–123.

Received for review June 20, 2010. Accepted November 5, 2010.

JE100671V